LETTER Communicated by Jonathan Victor

Estimating the Temporal Interval Entropy of Neuronal Discharge

George N. Reeke
reeke@lobimo.rockefeller.edu
Allan D. Coop
adc@lobimo.rockefeller.edu
Laboratory of Biological Modelling, Rockefeller University, New York, NY 10021, U.S.A.

To better understand the role of timing in the function of the nervous system, we have developed a methodology that allows the entropy of neuronal discharge activity to be estimated from a spike train record when it may be assumed that successive interspike intervals are temporally uncorrelated. The so-called interval entropy obtained by this methodology is based on an implicit enumeration of all possible spike trains that are statistically indistinguishable from a given spike train. The interval entropy is calculated from an analytic distribution whose parameters are obtained by maximum likelihood estimation from the interval probability distribution associated with a given spike train. We show that this approach reveals features of neuronal discharge not seen with two alternative methods of entropy estimation. The methodology allows for validation of the obtained data models by calculation of confidence intervals for the parameters of the analytic distribution and the testing of the significance of the fit between the observed and analytic interval distributions by means of Kolmogorov-Smirnov and Anderson-Darling statistics. The method is demonstrated by analysis of two different data sets: simulated spike trains evoked by either Poissonian or near-synchronous pulsed activation of a model cerebellar Purkinje neuron and spike trains obtained by extracellular recording from spontaneously discharging cultured rat hippocampal neurons.

1 Introduction

Spike trains generated by the discharge activity of neurons are composed of sequences of action potentials (spikes or impulses) that are generally accepted as providing the predominant mode of communication between neurons within the central nervous system (Perkel, 1970). Classically, the rate-coded properties of a spike train have been considered most important, for example, when sensory stimulus intensity is taken to be represented by the mean spike rate in a particular fiber or group of fibers (Adrian, 1928).

However, a significant feature of neuronal discharge activity, particularly within the cortex, is its high variability (Buracas, Zador, DeWeese, & Albright, 1998; Noda & Adey, 1970; Shadlen & Newsome, 1998; Softky & Koch, 1993; Tolhurst, Movshon, & Dean, 1983; Whitsel, Schreiner, & Essick, 1977). Although less widely accepted, the presence of discharge variability suggests that the timing of neuronal impulses as well as only their rate may be important (Segundo, 2000), and numerous alternatives to rate coding have been proposed (Buzsáki, Llinás, Singer, Berthoz, & Christen, 1994; Eggermont, 2001; Gilbert, 2001; Meister & Berry, 1999; Perkel & Bullock, 1968). In many cases, analysis is based on the temporal dispersion or pattern of neuronal discharge within a spike train, measures of which include the standard deviation (SD), coefficient of variation (CV = SD/mean), serial correlation of intervals, features of burst discharge such as the spike number and burst duration (e.g., Lisman, 1997), or metric-space techniques (Victor & Purpura, 1996). In contrast with the classical rate-based approach, the characteristic feature of such temporal coding is the importance of the exact time at which neuronal discharge occurs.

A theoretically grounded measure of the weighted average probability of individual alternative events, the entropy, originated in statistical mechanics and is fundamental to communication theory (Segundo, 1970; Shannon & Weaver, 1949). This measure has subsequently been adapted (see, e.g., Brillouin, 1962; MacKay & McCulloch, 1952; Rieke, Warland, de Ruyter van Steveninck, & Bialek, 1997) to provide the necessary foundation for estimation of the transmission of information within (Manwani & Koch, 2000) and between neurons (e.g. Bialek, Rieke, de Ruyter van Steveninck, & Warland, 1991; Borst & Theunissen, 1999; Brecht, Goebel, Singer, & Engel, 2001; Brenner, Strong, Koberle, Bialek, & de Ruyter van Steveninck, 2000; Buracas & Albright, 1999; Buracas et al., 1998; Butts, 2003; deCharms & Zador, 2000; Dimitrov & Miller, 2001; Eckhorn & Pöpel, 1974; Gershon, Wiener, Latham, & Richmond, 1998; Liu, Tzonev, Rebrik, & Miller, 2001; Optican & Richmond, 1987; Reich, Mechler, Purpura, & Victor, 2000; Rieke et al., 1997; Stein, 1967; Szczepanski, Amigó, Wajnryb, & Sanchez-Vives, 2003; Werner & Mountcastle, 1965; Wiener & Richmond, 1999). One feature of the methodologies employed in many of these reports is their emphasis on the analysis of signal transmission following the sensory stimulation of visual pathways. Here, however, we are specifically concerned with estimating the entropy of individual spike trains, regardless of their dependence on any particular sensory stimulus.

With the content and mechanisms of neural coding still in dispute (see, e.g., Eggermont, 1998; Friston, 1997), the estimation of entropy becomes more uncertain as neuronal impulse activity propagates from primary sensory areas to multi- and supramodal cortical areas. In part, this is due to difficulties in identifying the set of possible signals from which a particular neuronal response is selected and thus the probability with which a given response occurs. This is compounded by the lack of suitable experimental

preparations capable of providing data sets of the length required to establish good estimates of the event probabilities underlying the calculated entropy.

Here we describe the analytic distribution method (for convenience, the interval method) for the calculation of the temporal interval entropy or simply the interval entropy of a neuronal signal. The name *interval entropy* is proposed because probability estimates are based on hypothetical sets of all possible spike trains having the same distribution of interspike intervals as the spike train in question. The methodology requires no knowledge of stimulus properties and is applicable to individual spike trains. It is based on the interspike interval distribution obtained from a particular spike train and involves calculation of the entropy of an equivalent continuous analytic distribution as a means of accomplishing extrapolation to large data record lengths. In the following sections, the interval methodology is described and then applied to analyze spike trains obtained from two different sources. Our primary purpose is to demonstrate the methodology rather than to identify the functional relevance of any spike train properties that may be revealed by the analyses. Initially, artificially generated spike trains are analyzed. Results of these analyses are compared with entropy estimates for the same spike trains obtained with either the direct method (de Ruyter van Steveninck, Lewen, Strong, Koberle, & Bialek, 1997; Strong, Koberle, de Ruyter van Steveninck, & Bialek, 1998) or the non-parametric method of Kozachenko and Leonenko (1987). We also apply the interval methodology to spike trains obtained via extracellular single unit recording of spontaneous discharge activity from acutely dissociated, cultured rat hippocampal neurons.

2 Previous Entropy Measures

It has previously been suggested that entropy may provide a sensitive measure for quantification of neuronal discharge variability (Sherry & Klemm, 1981). One of the simplest approaches to the analysis of neuronal discharge entropy relies on a rate-based description of the neural code. Here, the fundamental event is assumed to be the action potential (or spike), and the entropy depends on the neuronal discharge rate. When N different spike signals are equally likely, that is, the probability of each signal is $1/N$, the entropy, H, is given by the relation $H = \log_2 N$ (Hartley, 1924). Alternatively, the Shannon formulation derives a measure of the entropy of a signal from estimates of the probabilities that particular signals would be observed if drawn at random from among a finite set of all possible signals that might be emitted under a given set of conditions. It is given in the discrete case by

$$H = -\sum_{i=1}^{N} p_i \log_2 p_i, \tag{2.1}$$

where p_i is the probability of the ith event, N the total number of events, and $\sum p_i = 1$. Equation 2.1 naturally generalizes to the case of a continuous range of values to give the so-called differential entropy function,

$$H(X) = -\int_S f(x) \log_2 f(x)\, dx,$$

where S is the support set of X with a density $f(x) > 0$. From $H(X)$, the discrete entropy can be calculated by

$$H_\Delta(X) = H(X) - \log_2 \Delta t, \tag{2.2}$$

where Δt is the temporal bin width (Cover & Thomas, 1991). Several complementary methods are currently available that, via various simplifying assumptions, allow upper or lower bounds of spike train entropy to be estimated (reviewed by, e.g., Borst & Theunissen, 1999).

One rate-based measure originates in a derivation of the Shannon entropy function (see equation 2.1) in which a binary representation of a spike train is obtained by dividing the time axis into discrete bins of width Δt. Each bin is coded as 1 if a spike is present in that bin and 0 otherwise (Brillouin, 1962; MacKay & McCulloch, 1952). The observed spike train is taken to have been selected from the set of all possible spike trains with the same number of 1s and 0s. This approach has been developed by various simplifying assumptions to give the mean rate entropy in bits per spike as a function of Δt (from Rieke et al., 1997)

$$H_R \approx \log_2 \left(\frac{e}{\bar{r}\Delta t} \right), \tag{2.3}$$

where e is the base of natural logarithms, $\bar{r}$ is the mean spike rate, and it is assumed that the probability of finding a spike in any one bin is $\ll 1$. Here, H_R is referred to as the rate entropy and is given as the mean entropy in bits per spike. It provides an upper bound to the entropy for a given activation rate and choice of Δt.

2.1 The Direct Method. As an example of a methodology for measuring entropy that takes into account both spike timing and any correlations that may be present within sequences of intervals, we briefly summarize the entropy estimation component of the so-called direct method of spike train analysis (de Ruyter van Steveninck et al., 1997; Strong et al., 1998). The direct method begins, like the calculation of the rate entropy H_R, with a binary representation of the given spike train in bins of width Δt. Consecutive bins (or "letters") are grouped into "words" of L bins. For a given word length L and resolution Δt, the entropy of the response to a particular stimulus in bits per second is obtained from the probability distribution of the observed

words by application of

$$H_D(L, \Delta t) = -\frac{1}{L\Delta t} \sum_{w \in W(L,\Delta t)} p(w) \log_2 p(w), \tag{2.4}$$

where w is a specific word (spike pattern), $W(L, \Delta t)$ the set of all possible words comprising L bins of width Δt, and $p(w)$ is the probability of observing pattern w in the spike train. The true entropy for a given measurement precision can be obtained only when observation times are sufficiently long to obtain accurate estimates of $p(w)$ and after extrapolation of $H_D(L, \Delta t)$ to infinite L. In one version of this method, which is used for the calculations reported here, H_D is plotted versus $1/L$, the point of minimal fractional change in slope is found, and the four values of L up to and including this point are used for the extrapolation (Reinagel, Godwin, Sherman, & Koch, 1999). H_D may then be divided by the mean spike rate to give an estimate of the mean entropy in bits per spike.

The advantage of the direct method is that it makes no prior assumptions about the distribution of letters in a word or about the nature of the stimulus. However, as is generally the case for accurate estimation of spike train entropy, application of the method faces three obstacles (Optican, Gawne, Richmond, & Joseph, 1991). First, it is not always clear how to make a principled choice for the temporal resolution at which a spike train should be discretized. This is referred to here as the binning problem. Second, responses to a stimulus often appear to be highly variable (but see Reinagel & Reid, 2002). Third, experimental considerations frequently limit the sample size. The impracticality of collecting the large data sets required to estimate the occurrence probability of word patterns accurately, particularly long ones, is referred to here as the sampling problem.

2.2 The KL Method. A nonparametric method of entropy estimation has been proposed by Kozachenko and Leonenko (1987). Based on the method of Dobrušin (1958), it provides an asymptotically unbiased estimator that gives the entropy of a continuous random vector from a sample of independent observations. For convenience, it is referred to here as the KL method and provides an entropy estimate referred to as the KL entropy (H_{KL}). (H_{KL} should not be confused with the similarly named relative entropy or Kullback-Leibler distance, which may be calculated for two probability mass functions; e.g., Cover & Thomas, 1991). In brief, let R^m be the m-dimensional Euclidean space with metric

$$\rho(x_1, x_2) = \left\{ \sum_{j=1}^{m} (x_1^{(j)} - x_2^{(j)})^2 \right\}^{1/2},$$

where $x_i = (x_i^{(1)}, \ldots, x_i^{(m)}) \in R^m$, $i = 1, 2$, and $m \geq 1$. From the sample $X_1, \ldots, X_N$, $N \geq 2$, compute $\rho_i = \min\{\rho(X_i, X_j), j \in 1, 2, \ldots, N\}\backslash\{i\}\}$ and let

$$\bar{\rho} = \left\{ \sum_{i=1}^{N} \frac{\rho_i}{\Delta t} \right\}^{1/N}, \tag{2.5}$$

where Δt is a bin width introduced to make $\bar{\rho}$ a dimensionless quantity. The entropy may then be obtained in bits per interval from

$$H_{KL} = \left(\frac{1}{\ln 2} \right) [m \ln \bar{\rho} + \ln c_1(m) + \ln \gamma + \ln(N-1)], \tag{2.6}$$

where

$$c_1(m) = \frac{\pi^{m/2}}{\Gamma(\frac{m}{2}+1)},$$

$m = 1$ for all analyses reported here, $\ln \gamma = 0.577216$ (the Euler constant), and $\Gamma(\bullet)$ is the gamma function.

In some runs (see section 4), the temporal resolution of spike timing was increased to that of the double floating-point number precision of MATLAB by the addition of uniform noise to each interval in a spike train. The noise was constrained such that interval durations were randomly varied within the 10 μs simulation resolution. Under this condition, all intervals contributed to the estimate of H_{KL}. With the exception of the lower curves in Figures 3A and 3B, all values reported for the KL entropy were obtained as the mean of 10 replicates for each data set where the random number seed used to generate the noise was different in each analysis.

3 Methods

3.1 The Interval Method. Based on the assumption that temporal precision may typically provide a more important limiting factor on information transmission than maximum impulse rate, an early theoretical study concluded that interval modulation provides a more efficient mode of encoding than purely rate-based modulation (MacKay & McCulloch, 1952). Although subsequent studies of interspike interval distributions obtained from spontaneously discharging neurons in slice preparations of rat cerebellar cortex showed that serial correlation of adjacent intervals may extend over clusters of up to three to five intervals (Klemm & Sherry, 1981; Sherry & Klemm, 1981), for simplicity, the interval method given here assumes independence of successive intervals, as does the KL methodology.

The interval method proceeds by assuming that (1) a spike train consists of a sequence of symbols composed of interval spike pairs where each temporal interval following the first spike is terminated by the occurrence of a spike, (2) the set of possible signals from which an observed spike train

is drawn is the set of all spike trains with the same distribution of interspike intervals, (3) the distribution of spike intervals in an arbitrarily long spike train can be obtained by maximum likelihood estimation (MLE) of the parameters that match a suitably chosen analytical distribution to an observed sample of that spike train, and (4) the entropy determined by the timing of neuronal discharge can be calculated from the continuous probability distribution for an appropriate choice of resolution, Δt. (See the end of the following section.)

3.1.1 Estimating the Interval Entropy (H_I). The interval methodology avoids the binning problem by obtaining with MLE techniques the parameter values for the underlying continuous distribution from which the intervals of a particular spike train are most likely to have been drawn. The entropy may then be obtained by analytic or numeric techniques from the continuous distribution at any desired temporal resolution.

Within the context of spike train analysis, several different approaches have been formulated to address the sampling problem, that is, the estimation of a probability function from a finite sample size, and different correction factors have been proposed (Optican et al., 1991; Panzeri & Treves, 1996; Sanderson & Kobler, 1976; Wolpert & Wolf, 1995). Here, the sampling problem is addressed by employing a best-fit analytic distribution to approximate the limit of an infinitely long data set. This approach has the advantage that the spike train duration required to provide sufficient data can be estimated by noting where the entropy estimates obtained from analytic probability density function fit to records of increasing durations asymptote to a constant value, with no further correction for undersampling required.

The interval method is not limited to a particular analytical density function; any suitable function or combination of functions may be employed to estimate the interval probability density of a given spike train. A sum of functions may be particularly useful when a neuron exhibits periodic burst discharge, a condition under which the observed interval probability density may contain multiple peaks.

In the analyses reported here, typically one or both of two analytic probability density functions are employed: the generalized gamma distribution or the gaussian distribution. The generalized gamma distribution, in the case of a neuron exhibiting an absolute refractory period, requires a three-parameter form of the probability density function given by

$$\gamma(x; a, s, \tau) = \frac{(x-s)^{a-1}}{\tau^a \Gamma(a)} e^{\frac{-(x-s)}{\tau}}, (x \geq s \geq 0; a, \tau > 0), \tag{3.1}$$

where a is the order or shape parameter and s and τ gave the time axis shift and the time scaling parameters of the distribution, respectively. This distribution is chosen as it is characteristic of simple models of neural spike production (see, e.g., Usher, Stemmler, & Koch, 1994) and because of its rela-

tion to the Poisson distribution when $a = 1$. Early studies reported excellent fits between neuronal discharge activity and the gamma distribution (Stein, 1965), as have others since (e.g., Tiesinga, José, & Sejnowski, 2000). In any event, this distribution appears to be justified heuristically by its ability to fit distributions that range from exponential to near gaussian as the order parameter, a, is increased.

When all three parameters of a gamma distribution are unknown, an efficient method of parameter estimation is that of MLE (Mann, Schafer, & Singpurwalla, 1974). MLE values are estimated from the observed distribution, O, by maximizing the likelihood function

$$L = \prod_i p(x_i),$$

where in the gamma case

$$p(x_i) = \gamma(x_i; a, s, \tau)$$

for unimodal distributions and

$$p(x_i) = f\gamma_1(x_i; a_1, s_1, \tau_1) + (1 - f)\gamma_2(x_i; a_2, s_2, \tau_2)$$

for bimodal distributions. In the bimodal case, f is a constant ($0 < f < 1$) that distributes the analytic probability between the two peaks in O, and a_1 and a_2, s_1 and s_2, and τ_1 and τ_2 are the order, shift, and scaling parameters, respectively, of the two density functions as determined by the MLE procedure.

It is often computationally advantageous to maximize the log likelihood instead of the likelihood function. Thus, for the unimodal case,

$$\ln L = \sum_i \ln[\gamma(i)], \tag{3.2}$$

and the bimodal case,

$$\ln L = \sum_i \ln[f\gamma_1(i) + (1 - f)\gamma_2(i)] \tag{3.3}$$

where

$$\gamma_n(i) = \left[\frac{(x_i - s_n)^{a_n - 1}}{\tau_n^{a_n}\Gamma(a_n)}\right] e^{\frac{-(x_i - s_n)}{\tau_n}}, n = 1, 2.$$

The extension to more than two component distributions is obvious.

Once the parameters a, s, and τ are known, the entropy of the fitted gamma distribution can be calculated by summation of the Shannon entropy function (see equation 2.1), where for the unimodal case, the probability that an interspike interval lies in the interval $x = [i\Delta t, (i + 1)\Delta t]$ is given by

$$p_i = [Q((i + 1)\Delta t; a, s, \tau) - Q(i\Delta t; a, s, \tau)] \tag{3.4}$$

where i gives the bin number, Δt the bin width, and Q is the incomplete gamma function,

$$Q(x; a, s, \tau) = \gamma\left(\frac{x-s}{\tau}, a\right) \equiv \frac{1}{\Gamma(a)} \int_0^{\left(\frac{x-s}{\tau}\right)} t^{a-1} e^{-t}\, dt,$$

or analytically (see equation 2.2) where

$$H_\Delta(X) = \left(\frac{1}{\ln 2}\right)\left[\ln(\tau\Gamma(a)) + (1-a)\frac{\Gamma'(a)}{\Gamma(a)} + a\right] - \log_2 \Delta t, \tag{3.5}$$

and $\Gamma'(a)$ is the derivative of the gamma function.

For consistency with the bimodal case where the analytic entropy is not available in closed form (see below), the entropy of unimodal distributions is also obtained from equation 2.1. To keep the set of possible messages finite (Shannon, 1948), the summation is truncated after N terms, when the p_i are sufficiently small to achieve numerical convergence (we use $1 - \sum p_i < 1 \times 10^{-8}$).

In the absence of an analytic expression for $H(X)$ in the bimodal case, the entropy is estimated from the Shannon entropy function (see equation 2.1), now using

$$\begin{aligned} p_i = {} & f[Q((i+1)\Delta t; a_1, s_1, \tau_1) - Q(i\Delta t; a_1, s_1, \tau_1)] \\ & + (1-f)[Q((i+1)\Delta t; a_2, s_2, \tau_2) - Q(i\Delta t; a_2, s_2, \tau_2)]. \end{aligned} \tag{3.6}$$

One or more gaussian distributions or a sum of gaussian and gamma distributions may provide an appropriate description when the order parameter, a, of a gamma distribution becomes large, although we note that the matching of single gaussians to individual interval distributions obtained within the visual system has been unsuccessful (Berry, Warland, & Meister, 1997). The parameter values for the analytic gaussian probability density function,

$$G(x; m, \sigma) = \frac{1}{\sqrt{2\pi}\sigma} \exp\left(\frac{-(x-m)^2}{2\sigma^2}\right), (\sigma > 0), \tag{3.7}$$

from which the observed interval distribution, O, is most likely drawn, are obtained by MLE maximization of the log-likelihood function as given above for the gamma cases. In contrast with the gamma distribution, which extends over the range $[0, +\infty]$, the gaussian distribution extends over the range $[-\infty, +\infty]$. As the probability of negative temporal intervals has no meaning, such values are avoided by truncating the distribution at $x = 0$ by renormalization. If one defines

$$G_T(X) = \left(\frac{2}{\mathrm{erfc}(\frac{-m}{\sqrt{2}\sigma})}\right) G(x; m, \sigma), \tag{3.8}$$

where

$$\mathrm{erfc}(x) = \frac{2}{\sqrt{\pi}} \int_x^\infty e^{-t^2}\, dt$$

is the complementary error function, then

$$\int_0^\infty G_T(x)\, dx = 1 \text{ and } \sum_{i=0}^{N} G_T(x_i) \approx 1,$$

where N is chosen as given above such that $1 - \sum p_i < 1 \times 10^{-8}$.

An example of a more complex distribution is that of a comb function composed of multiple discrete gaussians, the amplitudes of which are constrained by a gamma envelope. Here,

$$P(x) = \left(\frac{1}{N_C}\right) \sum_{j=1}^{g} \left(\frac{\mu_j - s}{\tau}\right)^{a-1} e^{-\left(\frac{\mu_j - s}{\tau}\right)} e^{-\left(\frac{x-\mu_j}{2\sigma_j^2}\right)^2}, \tag{3.9}$$

where N_C is a normalization factor given by

$$N_C = \sqrt{\frac{\pi}{2}} \sum_{j=1}^{g} \left(\frac{\mu_j - s}{\tau}\right)^{a-1} e^{-\left(\frac{\mu_j - s}{\tau}\right)} \sigma_j \mathrm{erfc}\left(\frac{-\mu_j}{\sqrt{2}\sigma_j}\right),$$

g is the number of gaussian components within the gamma envelope, and μ_j is the mean of the jth gaussian ($\mu_j = s_0 + jT$), where s_0 is the offset of the first gaussian and T the temporal interval separating the means of each gaussian component. The entropy of such a function may then be obtained from equation 2.1, where the probability of the ith bin is

$$p(i) = \frac{1}{N_C} \sum_{j=1}^{g} \left(\frac{\mu_j - s}{\tau}\right)^{a-1} e^{-\left(\frac{\mu_j - s}{\tau}\right)} \times \sqrt{\frac{\pi}{2}} \left[\mathrm{erf}\left(\frac{(i+1)\Delta t - \mu_j}{\sqrt{2}\sigma_j}\right) - \mathrm{erf}\left(\frac{i\Delta t - \mu_j}{\sqrt{2}\sigma_j}\right)\right]. \tag{3.10}$$

Because in multimodal cases the integral is not always available in closed form, summation is carried out over bins explicitly, a procedure that is equivalent to equation 2.2 in the limit of small Δt. The continuous distribution is divided into bins of width Δt, and the probability of each bin is calculated as a definite integral of the underlying continuous distribution over the width of the bin. The Shannon entropy (see equation 2.1) is calculated from the resulting bin probabilities p_i. If a distribution spans only a small number of bins, Δt, the entropy may be calculated for a reduced bin width and then

converted to that of the required bin width from

$$H(\Delta t_2) = H(\Delta t_1) - \log_2\left(\frac{\Delta t_2}{\Delta t_1}\right), \tag{3.11}$$

where Δt_1 and Δt_2 are the smaller and larger bin width, respectively.

Note that binning is not required to obtain the underlying probability distribution as the parameters of the analytic distribution are obtained by the MLE methodology. Thus, the assumption of a particular value of Δt for the entropy calculation plays no role in the determination of the analytic probability distribution $P(X)$.

Intuitively, there is a range of resolutions, Δt, at which the summation of the Shannon entropy function (see equation 2.1) might be performed, corresponding to the temporal resolution of the postsynaptic targets of the spike train. For the purpose of comparing the various entropy estimation methodologies, a bin width of 0.5 ms is employed here (Regehr & Stevens, 1999; Reinagel & Reid, 2000; Sabatini & Regehr, 1999).

3.1.2 Data Analysis. Analysis and fitting routines were developed by the authors in MATLAB Version 6.5 (MathWorks Inc., Natick, MA. http://www.mathworks.com). A MATLAB-supplied function that implements the Nelder-Mead simplex direct search algorithm, *fminsearch*, was employed to perform the fits. To enforce the requirement $s_n \geq 0$ (see equation 3.1), this variable is transformed to a variable β,

$$\beta = -\ln\left(\frac{x_{\min} - s - \varepsilon}{x_{\min}}\right), -\infty \leq \beta \leq \infty, \tag{3.12}$$

where $x_{\min}$ is the smallest interval in O and ε gives the tolerance to which $(x_{\min} - s)$ approaches zero (we use, $\varepsilon = 1 \times 10^{-8}$). During the MLE procedure, β is allowed to vary freely. The true value of s is recovered following parameter estimation via the inverse transformation,

$$s = x_{\min}(1 - e^{-\beta}) - \varepsilon. \tag{3.13}$$

Confidence intervals were obtained from suitable modifications of a MATLAB-supplied function, *mle*, which uses the input data and the parameter values of the MLE fit to calculate the Fisher information matrix, the inverse of which gives the covariance matrix of the parameter value estimates, θ. Confidence intervals, C_n (where n gives the magnitude of the confidence interval), are expressed as $\theta \pm c\nu$, where ν is the square root of the corresponding diagonal element of the inverse Fisher information matrix, and c is a constant that depends on the specific confidence interval required. For the analyses reported here, this was typically 99%, that is, $c = \sqrt{2}erf^{-1}(0.99)$. As entropy is determined by the variance of a distribution and is independent

of the mean (Rieke et al., 1997), m_n and s_n are not included in the values reported for confidence intervals.

3.2 Statistical Tests. The validity of the fit of each analytic distribution to the observed data was assessed by both the Kolmorogorov-Smirnov (KS; Press, Tevkolsky, Vetterling, & Flannery, 1992) and Anderson-Darling (AD; Anderson & Darling, 1954) statistical tests. The AD test is a modification of the KS test which increases the power of the KS test in the tails of a distribution. For each test, the probability (p_D and p_W for the KS and AD test, respectively) of obtaining values of the test statistic (D and W for the KS and AD test, respectively) that are equal to or greater in magnitude than the observed test statistic was calculated. A p-value close to zero indicates that a significant difference is likely to exist for the sample size used. Critical values for goodness-of-fit testing determined from estimated parameters must be calculated for each distribution, as under these circumstances, they are much smaller than tabulated values (e.g., Lilliefors, 1967), and in any event, values have not been tabulated for the composite distributions we used. As the parameters of an analytic distribution estimated by MLE from a given data set may be used directly (Kotz & Johnson, 1983), for each fit a number of intervals equal to the number in the observed data set are sampled with replacement from the analytic distribution and the appropriate test statistic is calculated. This procedure is repeated 5000 times to give a distribution of the test statistic from which critical and p-values may be obtained. When resampling from the comb function, the fractional contribution of each gaussian component is obtained from

$$f = \left(\frac{1}{N_C}\right)\sqrt{2\pi}\sigma_j\left(\frac{\mu_j - s}{\tau}\right)^{a-1} e^{-\left(\frac{\mu_j - s}{\tau}\right)}. \tag{3.14}$$

The validity of the MLE fits was also assessed qualitatively by visual comparison of the observed and analytic distributions and quantitatively by calculation of the root mean squared (RMS) error of the fit with the observed distribution. In both cases, cumulative interval distributions are constructed by assuming that intervals that varied by less than the recording resolution are equivalent. The RMS error, E, may then be obtained as

$$E = \left\{\frac{1}{N}\sum_{j=1}^{N}[O(x_j) - A(x_j)]^2\right\}^{1/2} \times 100\%, \tag{3.15}$$

where j ranges over the N observations included in the observed, O, and analytic, A, distributions. Additionally, many of the fits were also performed by direct minimization of E, with results similar to those obtained by MLE fitting. All entropy estimates are reported as the entropy per event where an event may be either a spike or an interval.

3.3 Source Data

3.3.1 Simulated Spike Trains. Spike trains were obtained from a model Purkinje neuron simulated at a temporal resolution of 10 μs (similar to that described by Coop & Reeke, 2001). Different discharge patterns were evoked by changing the number and activity of afferent (parallel fiber) synapses under two different stimulus paradigms. In the first, the Poissonian paradigm, impulse activity on each afferent fiber was generated as a Poisson point process with impulses temporally uncorrelated across the active fibers. In the second, the pulsed paradigm, the stimulus was composed of packets of pulses delivered at a fixed mean interpulse interval. Each packet was composed of impulses distributed as a truncated gaussian in time across the active afferent fibers with one impulse from the packet assigned at random to each fiber. The temporal jitter of the impulses within each pulse was controlled by varying the coefficient of variation (CV) of the gaussian (CV: 0.1 for the reported simulations). Paired-pulse facilitation following the model proposed by Atluri (1996) was included in the model PC. The number of active afferent fibers that contributed to each pulse controlled the rate and pattern of neuronal discharge. In both stimulation paradigms, the afferent pulse rate was held constant for the duration of a simulation.

3.3.2 Cultured Hippocampal Neurons. Extracellular simultaneous recordings of the spontaneous discharge of five hippocampal neurons were provided by E. Keefer of the Neurosciences Institute (San Diego, CA). These data were obtained from a culture of dissociated E18 rat hippocampal cells after 27 days in culture according to the basic methods of Ransom, Neale, Henkart, Bullock, & Nelson (1977) on a substrate-integrated 64-electrode array (Gross, Wen, & Lin, 1985). For recording, the electrode array was placed in a constant-temperature bath recording chamber and heated to 37°C. pH was maintained at 7.4 in a 90% air/10% CO_2 atmosphere. Neuronal activity was recorded with a two-stage, 64-channel amplifier system (Plexon Inc., Dallas, TX), and digitized simultaneously on a Dell 410 workstation. Spike identification and separation was accomplished with a template-matching algorithm (Plexon Inc.) in real time to provide single-unit spike timing data at a temporal resolution of 25 μs.

4 Results

4.1 Model Purkinje Cell. The essential features of the analytic distribution method are given in Figure 1 for simulated spike trains generated by either Poisson (see Figures 1A and 1C) or pulsed (see Figures 1B and 1D) stimulation at 8 impulses per second per afferent fiber. Under Poissonian stimulation, the model PC discharged at a rate of 56 spikes per second when contacted by 1000 afferent fibers. The interval probability distribution ob-

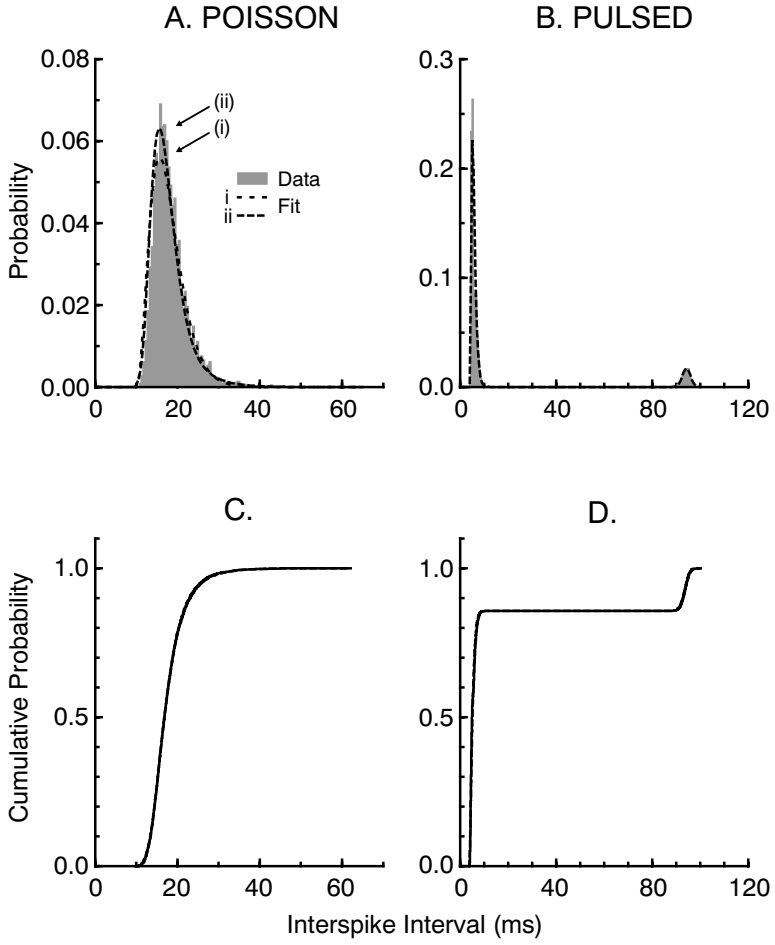

tained from a 100 s duration spike train was well fit (RMS error of fit: 1.7%) with a single gamma function to give an interval entropy, H_I, of 4.92 bits per interval (see Figure 1Ai). The shape and scale parameters for this fit were 3.9 ± 0.2 ($a \pm C_{0.99}$) and 2.0 ± 0.1($\tau \pm C_{0.99}$), respectively. Although for a bimodal gamma fit (see Figure 1Aii) the $C_{0.99}$ values were increased for the first ($a \pm C_{0.99}$: 5.7 ± 1.5, $\tau \pm C_{0.99}$: 1.3 ± 0.3 ms) and second ($a \pm C_{0.99}$: 1.5 ± 0.5, $\tau \pm C_{0.99}$: 4.4 ± 1.1 ms) gamma components, a lower RMS error (0.22%) suggested that this fit gave a better model of the data than the single gamma fit. This was confirmed by calculation of the p-values p_D and p_W, both of which were below 0.01 and above 0.99 for the single and double gamma fits, respectively. It was therefore concluded that the observed interval distribution was well described by the bimodal analytic distribution.

When this model was used to estimate the entropy of the given spike train, a slightly reduced value of 4.90 bits per interval was obtained for H_I.

Under an 8 impulse per second per fiber pulsed stimulus (CV: 0.1, i.e., SD of afferent impulse jitter was 12.5 ms around a 125 ms interpulse period) at a convergence of 800 afferent fibers, the model PC also discharged at 56 spikes per second. A reasonable fit to the interval data (RMS error 2.4%) was obtained with a bimodal distribution composed of a single gamma ($a \pm C_{0.99}$: 3.9 ± 0.2, $\tau \pm C_{0.99}$: 2.0 ± 0.1 ms) and a single gaussian distribution ($\sigma \pm C_{0.99}$: 1.7 ± 0.04). As both p_D and p_W were more than 0.99%, it was concluded that the observed interval distribution was not significantly different from the composite analytic distribution, and based on this fit, H_I was estimated to be 3.52 bits per interval.

We note that entropy estimates were also obtained from analytic distributions obtained by RMS error minimization. These values were little different (typically less than 2.5%) from those obtained with the MLE methodology.

The use of the best equivalent continuous distribution with the interval method allows good estimates of the entropy of neural discharge to be obtained from restricted data sets (as justified below, where interval entropy estimates from longer and shorter samples of the same data are compared with those obtained with the direct and KL methods). Further, the validity of the chosen data model can be quantified by the p-values obtained for the KS and AD statistics.

Figure 1: *Facing page*. The fit of analytic distributions by maximum likelihood estimation to observed interval data for simulated spike trains evoked in response to stimulation of a model Purkinje neuron. The stimulus had a mean rate per fiber of 8 spikes per second for both Poissonian (A, C) and pulsed (B, D) activation. By simulating 1000 afferent fibers in the Poissonian case and 800 in the pulsed case, we obtained a mean discharge rate of 56 spikes per second in both cases. The bin width of all histograms is 0.5 ms. (A) Interval probability distributions obtained from a 100 s spike train (binned histogram) appear to be well fit by either unimodal (i) or bimodal (ii) gamma distributions (dashed lines). (B) Interval probability distribution for a pulsed stimulus is well fit with a composite bimodal distribution comprising a single gamma and a single gaussian distribution (left and right peaks, respectively). The observed distribution is discontinuous in the range 10–90 ms where no intervals are observed (see *D*). (C) The bimodal gamma probability distribution (dashed line) obtained from the fit in *Aii* is shown as a cumulative interval histogram for comparison with the cumulative interval histogram constructed from the observed data (unbroken line). (D) The composite cumulative interval probability distribution (dashed line) obtained from the fit in *B* is shown for comparison with a cumulative interval histogram constructed from the observed data. Cumulative interval distributions are binned at the resolution of spike detection (10 μs). Note the two discrete peaks in the histogram and the absence of intervals in the range 10–90 ms.

To gain insight into the spike train duration required to ensure data adequacy, spike trains of increasing duration (up to 5000 s) were analyzed. As before, these spike trains were generated in response to 8 impulses per second per fiber Poissonian or pulsed stimulation. At a discharge rate of 6 spikes per second (750 and 270 afferent fibers, Poissonian and pulsed stimulation, respectively), the entropy estimate provided by each of the interval, KL, and direct methodologies typically stabilized within 10 to 40 s (see Figures 2A and 2B) (see below for comments about estimating H_{KL}). In

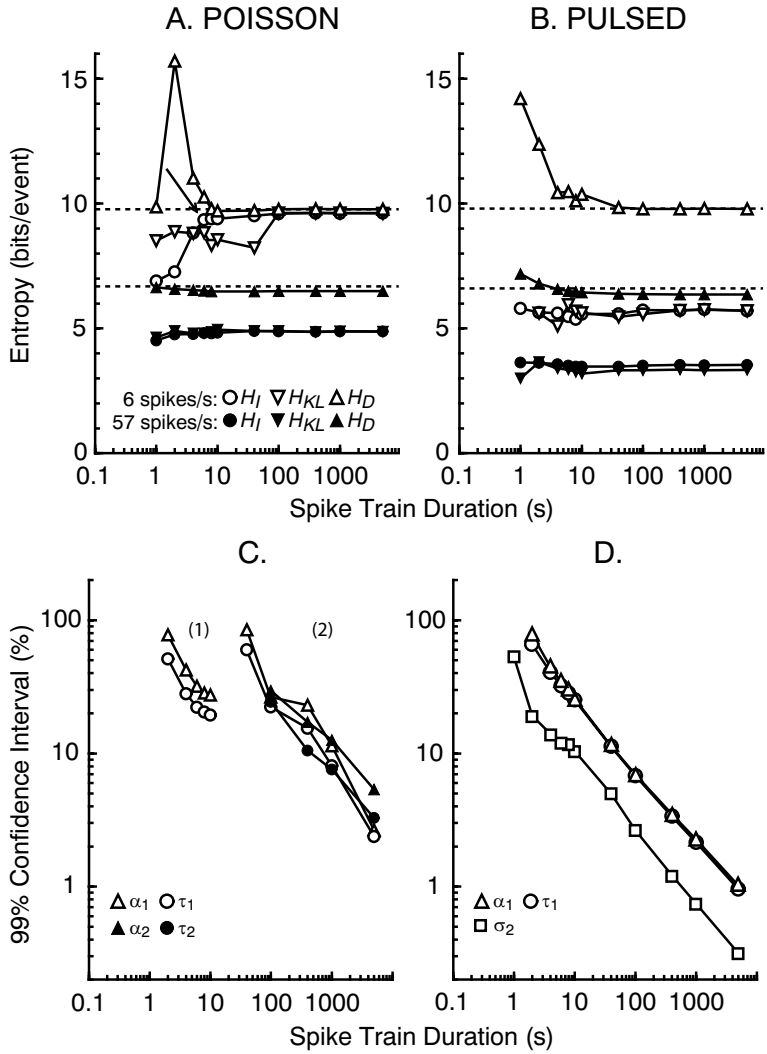

particular, good estimates of the entropy (within 1.6% to 2.7% of asymptotic values) were provided by the interval methodology with records as short as 6 s (see Figure 2A, arrow). At a discharge rate of 56 spikes per second (1000 and 800 afferent fibers, Poissonian and pulsed stimulation, respectively), H_I stabilized to within 0.5% to 1.7% of asymptotic values within 6 s, while all entropy estimates were close to their asymptotic values within 100 s of discharge (see Figures 2A and 2B). The discrepancy between H_R and H_D, on the one hand, and H_I and H_{KL}, on the other, for all cases except slow discharge under Poissonian stimulation is explored further below.

Figure 2 also shows the effect of increased spike train duration on the magnitude of $C_{0.99}$ values (given as a percentage of the associated parameter value estimate, i.e., $C_{0.99\%} = (c\nu/\theta) \times 100\%$) for the parameters of the analytic distribution used to calculate H_I. For both the uni- and bimodal fits

Figure 2: *Facing page*. Effect of spike train duration on the entropy magnitude calculated by three different methodologies for spike trains evoked at two different discharge rates under two different stimulation paradigms. (A) Entropy estimates obtained from spike trains evoked in response to 8 impulses per second per fiber Poissonian stimulation. At a discharge rate of 6 spikes per second (stimulation by 750 afferent fibers), entropy values estimated by the analytic distribution method (H_I), the direct method (H_D), and the Kozachenko-Leonenko method (H_{KL}), asymptoted to steady-state values with as little as 6, 8 and 100 s of data, respectively. At a discharge rate of 56 spikes per second (stimulation by 1000 afferent fibers), all three entropy estimates asymptoted to steady-state values within 10 s. Given sufficient data, the three entropy estimates obtained at a discharge rate of 6 spikes per second were all well matched to the predicted mean rate entropy, H_R (upper horizontal dashed line), whereas at 56 spikes per second only H_D agreed with the upper bound given by H_R (lower horizontal dashed line). (B) Entropy estimates obtained from spike trains evoked in response to 8 impulses per second per fiber pulsed stimulation. At a discharge rate of 6 spikes per second (stimulation by 270 afferent fibers) H_I, H_D, and H_{KL} asymptoted to steady-state values with spike train durations of 10–40 s, whereas at 56 spikes per second (stimulated by 800 afferent fibers) values asymptoted to steady-state values within 10 s. Given sufficient data, H_D again behaved similarly to the rate-based entropy estimator H_R (horizontal dashed lines). (C, D) Relationship between 99% confidence intervals (given as a percentage of the fit parameter value) obtained for the relevant MLE parameters of the analytic distributions fit to observed interval distributions as spike train duration was increased from 1 to 5000 s, for the Poissonian and pulsed stimulation paradigms, respectively. For spike train durations less than 40 s (in *C*), a single gamma function was sufficient to ensure no significant difference between the observed and analytic distributions, whereas for longer records, two gamma functions were required. Confidence intervals for the second gamma component of the 40 s record are not shown as they were above 100% (4513% and 1348% for α_2 and τ_2, respectively).

in Figures 2A and 2B, the $C_{0.99\%}$ values declined with increased spike train duration (see Figures 2C and 2D, respectively). It was notable that with short data records, although confidence intervals for the MLE estimated parameter values could be large, H_I entropy values were effectively asymptotic and p-values were large. For example, under Poissonian stimulation, a 100 s spike train with a mean rate of 56 spikes per second gave $C_{0.99\%}$ values of more than 20% (see Figure 2C), while H_I varied by less than 0.3% from its asymptotic value and both p_D and p_W were more than 0.99. Similarly, under pulsed stimulation for the same spike train duration but a two-component fit, $C_{0.99\%}$ values for the first and second components were more than 6% and 2.5%, respectively, while H_I varied by less than 0.4% from its asymptotic value and both p_D and p_W were also more than 0.99 (see Figure 2D). Overall, for H_I data shown in Figure 2A, the mean values of p_D and p_W were more than 0.37 for 6 spikes per second discharge and more than 0.68 for 56 spikes per second discharge, respectively. The equivalent p-values for pulsed stimulation were more than 0.57 and more than 0.95 for 6 and 56 spikes per second discharge, respectively (see Figure 2B).

The magnitude of the entropy obtained with the KL method (H_{KL}; Kozachenko & Leonenko, 1987) was sensitive to the absolute requirement for continuity of the observed interval distribution, and thus the computational resolution at which the discharge activity of the model PC was simulated. The KL method appeared to fail with small increases in PC discharge above the lowest rates observed (see Figure 3, empty circles). This failure was attributed to the reliance of the method on obtaining differences between intervals. Given the temporal resolution of the data (10 μs), as the regularity of discharge increased with increasing discharge rate, the number of intervals classed as identical also increased. Thus, under 64 spikes per second per fiber stimulation at a discharge rate of 68 spikes per second, only 20% and 14% of the intervals in the spike train were unique and could be used for the calculation of $\bar{\rho}$ (see equation 2.5) for Poissonian and pulsed stimulation, respectively.

A good match to the entropy estimates provided by the interval entropy, H_I, was obtained by artificially increasing the apparent temporal resolution at which simulated spike trains were recorded (see Figure 3, filled circles, and section 3). Thus, at a mean stimulus rate of 64 spikes per second per fiber, the percentage difference between H_I and H_{KL} was 0.89% and 1.7% for discharge rates of 2 to 141 and 10 to 163 spikes per second for Poissonion and pulsed stimulation, respectively. At higher and lower discharge rates, the difference between the two entropy estimates increased greatly, for example to 30% for discharge rates of 158 to 257 spikes per second in response to Poissonian stimulation, and more than 10% for discharge rates either less than 10 or more than 192 spikes per second. For discharge rates greater than 257 and 234 spikes per second under Poissonian and pulsed stimulation, respectively, the KL entropy was negative. For these reasons, the KL entropy was not explored further (see section 5).

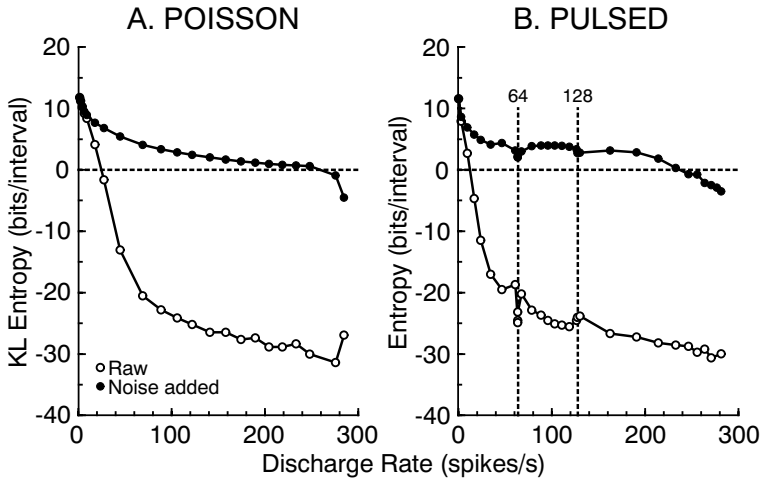

Figure 3: Effect of the addition of uniform noise to interval times contributing to entropy estimates provided by the method of Kozachenko and Leonenko (1987). The entropy values given in this figure were obtained by analysis of spike trains evoked by 64 impulses per second per fiber. The discharge rate was increased by increased afferent convergence. (A) Poissonian and (B) pulsed stimulation of the model Purkinje neuron. Entropy estimates obtained from computed interval data (open circles) were severely degraded regardless of the stimulation paradigm. Addition of uniform noise improved the apparent measurement resolution of the observed intervals. This satisfied the methodological requirement for continuity such that entropy estimates (see the filled circles) provided a reasonable match to those obtained with the interval method. All data in the upper curves (filled circles) were obtained from 10 replicate analyses where the random number seed generating the added noise was changed for each case.

We next used entropy measurements to explore the discharge behavior of the model PC in response to afferent stimulation at rates of 8, 64, and 128 impulses per second per afferent fiber where the mean impulse rate per second per fiber was held constant for the duration of each simulation and the rate of neuronal discharge was controlled by varying the number of active fibers.

Under Poissonian stimulation, an increase in the stimulus rate from 8 to 128 impulses per second per fiber had little influence on the calculated interval entropy, H_I, as under these conditions, the variability of the intervals in a spike train was proportional only to the discharge rate (not shown). As we have previously shown, frequency-locked discharge evoked by pulsed stimulation may be seen when afferent convergence is set such that a single action potential is evoked with each afferent stimulus pulse (Coop & Reeke,

2001). Here, this characteristic feature of spike trains seen for stimulation rates at 64 impulses per second per fiber or was lost with an increase in the stimulus rate to 128 impulses per second per fiber. Estimates of H_I obtained for spike trains generated in response to this stimulation rate were similar to those obtained for Poissonian activation (data not shown). This suggested that under these conditions, the PC was in a rate-coded regime, discharging independently of the temporal characteristics of the activation process. Analysis of the spike trains generated in response to 64 impulse per second per fiber is now presented as these data sets adequately display many of the features seen in response to lower stimulation rates.

In Figure 4 the entropies obtained with the H_R, H_D, and H_I methods for various discharge rates under both stimulation paradigms are compared. The values obtained for H_R (see Figures 4A and 4B, dashed lines) were of course identical. Those obtained for H_D (see Figures 4A and 4B, solid lines) under the two protocols were superimposable, thus confirming H_D to be a property of the spike train alone, independent of the stimulation paradigm (Strong et al., 1998).

Under the pulsed stimulation paradigm, both H_{KL} (see the filled circles in Figure 3B) and H_I (see the filled circles in Figure 4B) showed reductions at the locking frequency (stimulus rate = discharge rate) and at the frequency-halved and doubled rates of 32 and 128 spikes per second. However, both H_R and H_D failed to display sensitivity to these changes in the timing of cell discharge, which were attributable to the increased periodicity known to occur when each afferent pulse evokes a single action potential. To rule out data insufficiency as a source of this failure, a strictly periodic 64 spikes per second spike train was constructed. The respective H_D values obtained for this spike train were effectively identical at 6.251 to 6.250 bits per spike with an increase in spike train duration from 100 to 20,000 s. These values compared well with that of 6.248 bits per spike obtained when the duration of an equivalent frequency-locked spike train generated by the model PC was increased from 100 and 5000 s (discharge rates both 64.1 spikes per second) and were also concordant with the values obtained for an increase in spike train duration from 100 to 5000 s under Poissonian stimulation (mean discharge rates 63.7 and 63.4 spikes per second, H_D 6.257 and 6.265 bits per spike, for the respective spike train durations). We note that the change from Poissonian to pulsed stimulation typically decreased the spike train CV by a factor of five. Alternatively, analysis of the strictly periodic spike train for durations of 100 and 20,000 s with the interval methodology gave values of 0 bits per interval for H_I in both cases, as expected for application of Shannon theory to a strictly periodic signal.

At discharge rates higher than about 256 and 215 spikes per second under Poissonian and pulsed stimulation, respectively, the MLE methodology was unable to provide estimates of parameter values for analytic distributions that were not significantly different ($\alpha = 0.01, 0.05$) from the observed distributions. This failure was attributed to the presence of a 3.5 ms absolute

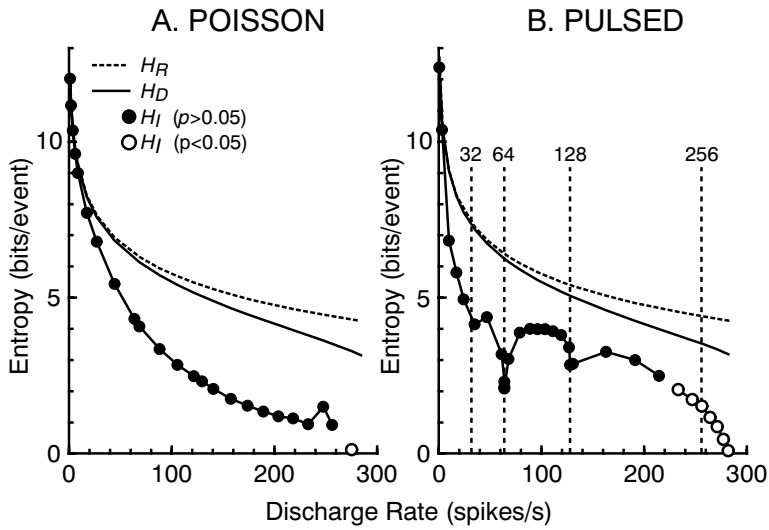

Figure 4: Comparison of the rate, H_R, direct, H_D, and interval, H_I, entropies, calculated for 100 s duration spike trains obtained from a model Purkinje neuron (PC) in response to stimulation at 64 spikes per second per afferent fiber. PC discharge rate was controlled by the number of active fibers (see the text for further details). (A) Poissonian stimulation. In comparison with estimates of H_I, which assumed intervals to be independent, estimates of H_D were considerably larger in magnitude for discharge rates higher than about 10 spikes per second. (B) Pulsed stimulation. In this case, the entropy provided by the direct method, H_D, did not appear to be sensitive to the changes in spike timing that occur under conditions of frequency locking where each pulse of afferent impulses evokes a single action potential and cell discharge becomes near periodic (vertical dashed lines at 32, 64, and 128 spikes per second discharge). The fact that the values of H_R and H_D remain effectively superimposed across the two stimulation paradigms tested suggests that unlike the entropy estimates provided by H_I, these measures fail to distinguish alterations in the temporal properties of the evoked discharge patterns. Filled circles indicate that fits of observed data to analytic distributions were not significantly different ($\alpha \leq 0.05$) by both the Kolmogorov-Smirnov and Anderson-Darling statistics. Open circles indicate the opposite. See the text for further details.

refractory period in the model PC, which provided an inflexible lower limit for the shortest interspike intervals. As the rate of PC discharge increased above 200 to 250 spikes per second, the observed interval distributions became more truncated to the left. The peak associated with this truncation could not be fit with the gamma and gaussian distributions employed. Although these peaks undoubtedly could have been well fit with one or more Dirac delta functions, this was not pursued.

In summary, the interval method appears to provide an entropy estimate that, under the assumption of independence, is quite sensitive to the distribution of intervals, whereas the direct method provides estimates that appear insensitive to changes in impulse timing as, for example, when the stimulation paradigm is changed from Poissonian to pulsed.

4.2 Cultured Hippocampal Neurons. To further demonstrate the interval methodology, the spontaneous discharge behavior of acutely dissociated, cultured hippocampal neurons was also analyzed. Spike train data were obtained simultaneously via extracellular recording (30 minute duration) from each of five neurons located in cultured slices from rat hippocampus area CA1. Discharge characteristics for each neuron and the results of three different entropy analyses are given in Table 1. By visual inspection, the interval histogram for each neuron appeared to be bimodal with preferred interval durations that represented mean spike rates of 9 and 70 spikes per second (not shown). However, the mean number of gamma and gaussian components fit with the interval methodology ranged from 4 to 6 (p_D and p_W both over 0.55).

As was the case for the simulated spike trains, the effect of spike train duration on entropy magnitude was assessed to determine whether in each case sufficient data were available to obtain a reliable entropy estimate for the hippocampal neurons. Results for cells 1, 2, and 3 are given in Figure 5 as their discharge rates spanned the range observed for the five neurons analyzed. In each case, the direct entropy, H_D, appeared to asymptote within 400 to 1000 s to the values calculated for the respective rate entropy estimates, H_R (see Figure 5A), whereas H_I and H_{KL} reached their asymptotic

Table 1: Characteristics of the Spontaneous Discharge of Five Acutely Dissociated Cultured Neurons Obtained from Rat Hippocampus Area CA1.

Neuron (No.)	Spikes (No.)	Rate (Spikes/s)	p_D	p_W	H_D (Bits/event)	H_I (Bits/event)	H_{KL} (Bits/event)
3	3519	2.0	0.90	0.90	11.44	10.28	10.24
4	4704	2.6	0.84	0.83	11.02	9.66	9.63
2	11,771	6.5	0.63	0.55	9.69	8.39	8.34
5	19,219	10.7	0.85	0.90	8.97	6.05	6.04
1	21,655	12.0	0.68	0.57	8.81	7.46	7.43

Notes: Data were obtained from simultaneous 30 minute duration recordings. The mean p-values for the Kolmogorov-Smirnov (p_D) and Anderson-Darling (p_W) statistical tests are given for the fits from which the interval entropy values plotted in Figure 5 were calculated. All entropies (H_D—direct, H_I—interval, and H_{KL}—Kozachenko and Leonenko entropies) were calculated with a bin width of 0.5 ms. H_{KL} was obtained as the mean of 10 replicates of each data set in which the random number seed for the added noise was varied. The entropy estimates obtained from the H_I and H_{KL} methods were quite similar, whereas, H_D differed from both of them.

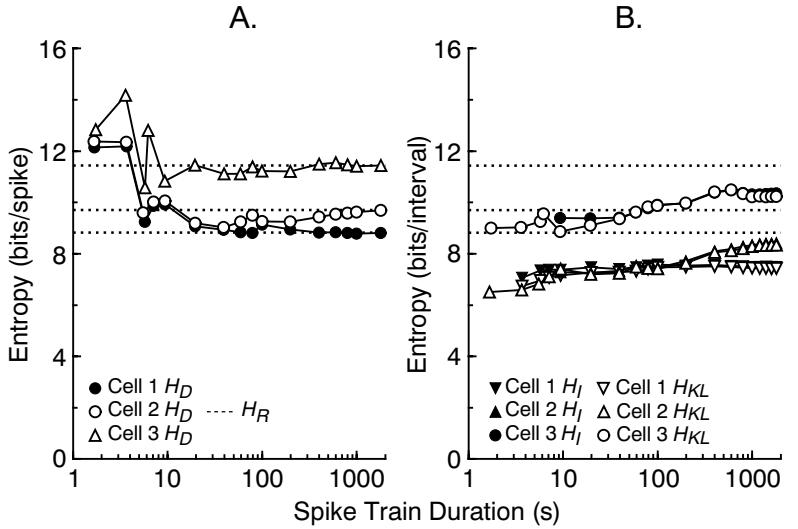

Figure 5: Entropy-based analysis of the extracellularly recorded spontaneous discharge of cultured rat hippocampus CA1 neurons of unknown type. (A) Comparison of entropy estimates obtained with the rate, H_R, and direct, H_D, methods from segments of various durations taken from 1800 s spike train records. H_D appears to asymptote to the value calculated for H_R. (B) Effect of spike train duration on the entropy estimated by the interval, H_I, and KL (H_{KL}; Kozachenko & Leonenko, 1987) methodologies. Both of these entropy estimates asymptote to constant values for spike train durations of 1000 s and longer. These asymptotic values are smaller than those obtained with H_D. Further details are given in Table 1 and the text.

values for spike train durations of about 1000 s or longer (see Figure 5B). As was the case for the simulated spike trains (see Figure 2A), here H_I and H_{KL} were characteristically smaller than H_D and H_R.

5 Discussion

The analytic distribution method for calculating the interval entropy provides a methodology that appears to be well suited for the quantification of the entropy of biological signals such as those embodied in spike trains. When applied to the interval data obtained from a spike train, the methodology determines the interval distribution from which an observed interspike interval distribution was most likely obtained. Characterization of the corresponding analytic distribution by an appropriate MLE procedure putatively gives the population of intervals predicted to occur in a spike train of effectively infinite duration exhibiting temporal properties statistically

indistinguishable from those of the observed spike train. The mean entropy per interval, H_I, can then be calculated at any desired temporal resolution, Δt, from the analytic distribution. For the purposes of this method, when applied to a spike train, the "symbol" of the Shannon formulation is taken to comprise the temporal interval between each pair of spikes and the spike that signals the completion of each interval. Thus, calculation of the mean entropy per interval for a given spike train serves to quantify an entropy associated with the timing of each action potential.

The interval methodology was developed in response to two problems associated with previous measures of entropy. The first is that of the sampling error introduced with the estimation of a suitable probability density function from a discrete sample. When neural discharge is assumed to provide the signaling element propagated within the neural code, it is not immediately obvious what distribution is appropriate a priori, particularly when no reasonable assumption on the prior is self-evident. This problem has been considered both generally (Wolpert & Wolf, 1995) and more recently for neural activity (Panzeri & Treves, 1996). However, as has been shown here for the interval method, it is relatively straightforward to choose empirically a continuous function or combination of functions that describes the interval distribution obtained from a given spike train with a degree of precision better than that typically encountered for the experimental error associated with physiological experiments (less than 2% to 5%).

The second methodological improvement arises because for the interval method, the selection of the temporal resolution for the entropy calculation is decoupled from the determination of the interspike interval distribution. Unlike previous methods, for which the choice of bin width Δt for digitization of the spike train also provides the resolution at which the entropy calculation is made, by employing MLE techniques to obtain the underlying probability distribution from which the population of observed intervals is most likely obtained, the interval method does not rely on a binning procedure. This allows the resolution of the entropy estimate to be independent of the estimation of the parameters of the continuous distribution from which it is obtained. This step may therefore be based on relevant principles other than those used to select an observational bin width.

Other novel features of the interval method are related to quantification of the validity of the entropy estimate. They include confidence intervals on the parameters obtained for the analytic distribution, the availability of the RMS error obtained from the fit between the observed and the analytic distribution, and statistical testing of the fit between the observed and analytic distributions.

Although confidence intervals were relatively large for the 100 s spike train durations employed in our analyses, entropy estimates typically asymptoted to a constant value prior to the smaller confidence intervals obtained as spike train duration was increased. Large values of the RMS error may be used as an internal indicator of situations in which the method

may not be applied with confidence. Further, visual comparison of the discrete and continuous probability distributions typically indicates whether the error is due to an incorrect choice of the analytic distribution, or, with an appropriate choice, whether the error is either uniformly distributed across all interval durations or localized. Thus, data about which interval durations exhibit anomalous behavior become available. When taken together with the availability of statistical tests suited to determining the validity of the fit between the observed and fit distributions, the usefulness of the methodology is greatly enhanced. In particular, calculation of both the KS statistic, D, and the AD statistic, W, provide both quantification and localization of any anomalies—at the median or the tails of a distribution for the KS and AD test, respectively.

The nonparametric estimator provided by Kozachenko and Leonenko (1987), while at first appearing attractive, was problematic when applied to neuronal data. This was attributed to the strict requirement for continuity, which was not satisfied even at temporal resolutions of 10 μs. (We note in passing that this characteristic of the KL entropy might advantageously be employed to detect discretization of interval data.) Analyses could be performed by adding uniform noise to the intervals in an observed distribution, a procedure that artificially increased the measurement resolution. This was particularly the case when an interval distribution contained a sharp shoulder, for example, at higher discharge rates when interval durations were limited by the absolute refractory period. Ideally, the observed distribution could be generated by resampling from an appropriate analytic distribution, obtained, for example, by the interval methodology outlined here. This data set would then provide sufficient resolution to estimate the KL entropy. The disadvantage with this approach is that crucial steps required to estimate H_{KL} are also those required for estimating the interval entropy, H_I, with the entropy in both cases determined by the validity of the analytic distribution obtained. Further, the requirement for continuity of the distribution for the KL method would appear to preclude resampling techniques to obtain confidence intervals on the KL entropy estimate. Finally, the KL method provides a single entropy value that is devoid of the mechanistic insights that may be obtained using the interval methodology.

We now turn to a comparison of the interval and direct methodologies. Here it was notable that, as might be predicted, the two methodologies gave entropy estimates in good agreement at low discharge rates when the activation process was Poissonian and interspike intervals could be assumed to be independent events. Nonetheless, it should be understood that the basic assumptions of the two methods regarding the nature of the fundamental signaling event are different, and so the results cannot be expected to agree in all cases. This was particularly apparent as the periodicity of neuronal discharge increased near the locking frequency under a pulsed stimulation paradigm. In this case, spike train entropy should be minimal

in accord with Shannon theory on the grounds of the low variability of interval duration and an increased correlation in interval sequences, both of which lower the number of messages that in principal could be conveyed by such spike trains. The apparent overestimation of H_D in such cases was attributed to the generation of novel words by the procedure of stepping the word bin-wise through the discretized spike train from an arbitrary origin. This increased the number of different word patterns observed in a spike train and led to a reduction in the probability attributed to any given spike or spike pattern and a consequent inflation of its contribution to the calculated entropy. The interval methodology avoids this problematic aspect of the direct method because intervals are assumed to be independent and, as might be considered appropriate for a biological context, no origin for the enumeration of different interval patterns needs to be defined.

Comparison of entropies obtained for spike trains of equivalent discharge rates but differing temporal patterns (as occurred when the stimulation paradigm was altered from Poissonian to pulsed) supported the proposition that the entropy estimate provided by the direct method was not sensitive to changes in spike timing. The fact that H_D appeared insensitive to interval correlations under conditions of near-periodic neuronal discharge suggests that this measure may be unfavorably biased when applied within a biological context.

Finally, because of its ability to quantify temporal aspects of neuronal discharge with a computationally convenient procedure that is effective with relatively short data records, we consider that the interval methodology shows considerable promise for analysis of both experimental and simulated spike trains.

Acknowledgments

This work was supported by Neurosciences Research Foundation. We thank E. Keefer of the Neurosciences Institute, San Diego, California, for supplying the data on cultured hippocampal neurons, V. Piëch for insightful discussion regarding implementation of the KL entropy calculations, and the anonymous referees for their helpful comments.

References

Adrian, E. D. (1928). *The basis of sensation*. New York: Norton.

Anderson, T. W., & Darling, D. A. (1954). A test of goodness of fit. *Journal of the American Statistical Association, 49*, 765–769.

Atluri, G. (1996). Determinants of the time course of facilitation at the granule cell to Purkinje cell synapse. *Journal of Neuroscience, 16*, 5661–5671.

Berry, M. J., Warland, D. K., & Meister, M. (1997). The structure and precision of retinal spike trains. *Proceedings of the National Academy of Sciences USA, 94*, 5411–5416.

Bialek, W., Rieke, F., de Ruyter van Steveninck, R. R., & Warland, D. (1991). Reading a neural code. *Science, 252*, 1854–1857.

Borst, A., & Theunissen, F. E. (1999). Information theory and neural coding. *Nature Neuroscience, 2*, 947–957.

Brecht, M., Goebel, R., Singer, W., & Engel, A. K. (2001). Synchronization of visual responses in the superior colliculus of awake cats. *Neuroreport, 12*, 43–47.

Brenner, N., Strong, S. P., Koberle, R., Bialek, B., & de Reuter van Steveninck, R. R. (2000). Synergy in a neural code. *Neural Computation, 12*, 1531–1552.

Brillouin, L. (1962). *Science and information theory* (2nd ed.). New York: Academic Press.

Buracas, G. T., & Albright, T. D. (1999). Gauging sensory representations in the brain. *Trends in Neuroscience, 22*, 303–309.

Buracas, T., Zador, A. M., DeWeese, M. R., & Albright, T. (1998). Efficient discrimination of temporal patterns by motion-sensitive neurons in primate visual cortex. *Neuron, 20*, 959–969.

Butts, D. A. (2003). How much information is associated with a particular stimulus? *Network: Computation and Neural Systems, 14*, 177–187.

Buzsáki, G., Llinás, R., Singer, W., Berthoz, A., & Christen, Y. (Eds.). (1994). *Temporal coding in the brain*. Berlin: Springer-Verlag.

Coop, A. D., & Reeke, G. N. (2001). Deciphering the neural code: Neuronal discharge variability is preferentially controlled by the temporal distribution of afferent impulses. *Neurocomputing, 38*, 153–157.

Cover, T. M., & Thomas, J. A. (1991). *Elements of information theory*. New York: Wiley.

de Ruyter van Steveninck, R. R., Lewen, G. D., Strong, S. P., Koberle, R., & Bialek, B. (1997). Reproducibility and variability in neural spike trains. *Science, 275*, 1805–1808.

deCharms, R. C., & Zador, A. (2000). Neural representation and the cortical code. *Annual Reviews in Neuroscience, 23*, 613–647.

Dimitrov, A. G., & Miller, J. P. (2001). Neural coding and decoding: Communication channels and quantization. *Network: Computation and Neural Systems, 12*, 441–472.

Dobrušin, R. L. (1958). A simplified method of experimentally evaluating the entropy of a stationary sequence. *Teoriya Veroyatnostei i ee Primeneniya, 3*, 462–464.

Eckhorn, R., & Pöpel, E. (1974). Rigorous and extended application of information theory to the afferent visual system of the cat. I. Basic concepts. *Kybernetik, 16*, 191–200.

Eggermont, J. J. (1998). Is there a neural code? *Neuroscience and Biobehavioral Reviews, 22*, 355–370.

Eggermont, J. J. (2001). Between sound and perception: Reviewing the search for a neural code. *Hearing Research, 157*, 1–42.

Friston, K. J. (1997). Another neural code? *NeuroImage, 5*, 213–220.

Gershon, E. D., Wiener, M. C., Latham, P. E., & Richmond, B. J. (1998). Coding strategies in monkey V1 and inferior temporal cortices. *Journal of Neurophysiology, 79*, 1135–1144.

Gilbert, C. D. (2001). The neural basis of perceptual learning. *Neuron, 31*, 681–697.
Gross, G. W., Wen, W., & Lin, J. (1985). Transparent indium-tin oxide patterns for extracellular, multisite recording in neuronal cultures. *Journal of Neuroscience Methods, 15*, 243–252.
Hartley, R. V. L. (1924). Transmission of information. *Bell System Technical Journal, 7*, 535.
Klemm, W. R., & Sherry, C. J. (1981). Serial ordering in spike trains: What's it "trying to tell us"? *International Journal of Neuroscience, 14*, 15–33.
Kotz, S., & Johnson, N. L. (Eds.). (1983). *Encyclopedia of statistical sciences*. New York: Wiley.
Kozachenko, L. F., & Leonenko, L. (1987). Sample estimate of the entropy of a random vector. *Problems of Information Transmission, 23*, 95–101.
Lilliefors, H. W. (1967). On the Kolmorogorov-Smirnov test for normality with mean and variance unknown. *Journal of the American Statistical Association, 62*, 399–402.
Lisman, J. E. (1997). Bursts as a unit of neural information: Making unreliable synapses reliable. *Trends in Neuroscience, 20*, 38–43.
Liu, R. C., Tzonev, S., Rebrik, S., & Miller, K. D. (2001). Variability and information in a neural code of the cat lateral geniculate nucleus. *Journal of Neurophysiology, 86*, 2789–2806.
MacKay, D. M., & McCulloch, W. S. (1952). The limiting information capacity of a neuronal link. *Bulletin of Mathematical Biophysics, 14*, 127–135.
Mann, N. R., Schafer, R. E., & Singpurwalla, N. D. (1974). *Methods for statistical analysis of reliability and life data*. New York: Wiley.
Manwani, A., & Koch, C. (2000). Detecting and estimating signals over noisy and unreliable synapses: Information-theoretic analysis. *Neural Computation, 13*, 1–33.
Meister, M., & Berry, M. J. II. (1999). The neural code of the retina. *Neuron, 22*, 435–450.
Noda, H., & Adey, W. R. (1970). Firing variability in cat association cortex during sleep and wakefulness. *Brain Research, 18*, 513–526.
Optican, L. M., Gawne, T. J., Richmond, B. J., & Joseph, P. J. (1991). Unbiased measures of transmitted information and channel capacity from multivariate neuronal data. *Biological Cybernetics, 65*, 305–310.
Optican, L. M., & Richmond, B. J. (1987). Temporal encoding of two-dimensional patterns by single units in primate inferior temporal cortex. III. Information theoretic analysis. *Journal of Neurophysiology, 57*, 162–178.
Panzeri, S., & Treves, A. (1996). Analytical estimates of limited sampling biases in different information measures. *Network: Computation and Neural Systems, 7*, 87–107.
Perkel, D. H. (1970). Spike trains as carriers of information. In F. O. Schmitt (Ed.), *The Neurosciences Second Study Program* (pp. 587–596). New York: Rockefeller University Press.
Perkel, D. H., & Bullock, T. H. (1968). Neural coding. *Neurosciences Research Program Bulletin, 6*, 221–348.
Press, W. H., Teukolsky, S. A., Vetterling, W. T., & Flannery, B. P. (1992). *Numerical Recipes in C* (2nd ed.). Cambridge: Cambridge University Press.

Ransom, B. R., Neale, E., Henkart, M., Bullock, P. N., & Nelson, P. G. (1977). Mouse spinal cord in cell culture. *Journal of Neurophysiology, 40*, 1132–1150.

Regehr, W. G., & Stevens, C. F. (1999). Physiology of synaptic transmission and short-term plasticity. In G. Stuart, N. Spruston, & M. Häusser (Eds.), *Dendrites* (pp. 135–175). New York: Oxford University Press.

Reich, D. S., Mechler, F. M., Purpura, K. P., & Victor, J. D. (2000). Interspike intervals, receptive fields, and information encoding in primary visual cortex. *Journal of Neuroscience, 20*, 1964–1974.

Reinagel, P., Godwin, D., Sherman, S. M., & Koch, C. (1999). Encoding of visual information by LGN bursts. *Journal of Neurophysiology, 81*, 2558–2569.

Reinagel, P., & Reid, R. C. (2000). Temporal coding of visual information in the thalamus. Journal of Neuroscience, 20, 5392-5400.

Reinagel, P., & Reid, R. C. (2002). Precise firing events are conserved across neurons. *Journal of Neuroscience, 22*, 6837–6841.

Rieke, F., Warland, D., de Ruyter van Steveninck, R. R., & Bialek, W. (1997). *Spikes: Exploring the neural code*. Cambridge, MA: MIT Press.

Sabatini, B. L., & Regehr, W. G. (1999). Timing of synaptic transmission. *Annual Reviews in Physiology, 61*, 521–542.

Sanderson, A. C., & Kobler, B. (1976). Sequential interval histogram analysis of non-stationary neuronal spike trains. *Biological Cybernetics, 22*, 61–71.

Segundo, J. P. (1970). Communication and coding by nerve cells. In F. O. Schmitt (Ed.), *The Neurosciences Second Study Program* (pp. 569–586). New York: Rockefeller University Press.

Segundo, J. P. (2000). Some thoughts about neural coding and spike trains. *BioSystems, 58*, 3–7.

Shadlen, M. N., & Newsome, W. T. (1998). The variable discharge of cortical neurons: Implications for connectivity, computation, and information coding. *Journal of Neuroscience, 18*, 3870–3896.

Shannon, C. E. (1948). A mathematical theory of communication. *Bell Systems Technical Journal, 27*, 379–423, 623–656.

Shannon, C. E., & Weaver, W. (1949). *The mathematical theory of communication*. Urbana: University of Illinois Press.

Sherry, C. J., & Klemm, W. R. (1981). Entropy as an index of the informational state of neurons. *International Journal of Neuroscience, 15*, 171–178.

Softky, W. R., & Koch, C. (1993). The highly irregular firing of cortical cells is inconsistent with temporal integration of random EPSPs. *Journal of Neuroscience, 13*, 334–350.

Stein, R. B. (1965). A theoretical analysis of neuronal variability. *Biophysical Journal, 5*, 173–194.

Stein, R. B. (1967). The information capacity of nerve cells using a frequency code. *Biophysical Journal, 7*, 797–826.

Strong, S. P., Koberle, R., de Ruyter van Steveninck, R. R., & Bialek, W. (1998). Entropy and information in neural spike trains. *Physical Review Letters, 80*, 197–200.

Szczepanski, J., Amigó, J. M., Wajnryb, E., & Sanchez-Vives, M. V. (2003). Application of the Lempel-Ziv complexity to the analysis of neural discharges. *Network: Computation and Neural Systems, 14*, 335–350.

Tiesinga, P. H. E., José, J. V., & Sejnowski, T. J. (2000). Comparison of current-driven and conductance-driven neocortical model neurons with Hodgkin-Huxley voltage-gated channels. *Physical Review E, 62*, 8413–8419.

Tolhurst, D. J., Movshon, J. A., & Dean, A. F. (1983). The statistical reliability of signals in single neurons in cat and monkey visual cortex. *Vision Research, 23*, 775–785.

Usher, M., Stemmler, M., & Koch, C. (1994). Network amplification of local fluctuations causes high spike rate variability, fractal firing patterns and oscillatory local field potentials. *Neural Computation, 6*, 795–836.

Victor, J. D., & Purpura, K. P. (1996). Nature and precision of temporal coding in visual cortex: A metric-space analysis. *Journal of Neurophysiology, 76*, 1310–1326.

Werner, G., & Mountcastle, V. B. (1965). Neural activity in mechanoreceptive cutaneous afferents: Stimulus response relations, Weber functions, and information transmission. *Journal of Neurophysiology, 28*, 359–397.

Whitsel, B. L., Schreiner, R. C., & Essick, G. K. (1977). An analysis of variability in somatosensory cortical neuron discharge. *Journal of Neurophysiology, 40*, 589–607.

Wiener, M. C., & Richmond, B. J. (1999). Using response models to estimate channel capacity for neuronal classification of stationary visual stimuli using temporal coding. *Journal of Neurophysiology, 82*, 2861–2875.

Wolpert, D. H., & Wolf, D. R. (1995). Estimating functions of probability distributions from a finite set of samples. *Physical Review E, 52*, 5841–6854.

Received March 13, 2002; accepted September 29, 2003.